ORIGINAL

Relationship between sodium-dependent phosphate transporter (NaPi-IIc) function and cellular vacuole formation in opossum kidney cells

Yuji Shiozaki[1], Hiroko Segawa[1], Saori Ohnishi[1], Akiko Ohi[1], Mikiko Ito[2], Ichiro Kaneko[1], Shinsuke Kido[3], Sawako Tatsumi[1], and Ken-ichi Miyamoto[1]

[1]*Department of Molecular Nutrition, University of Tokushima Graduate School, Tokushima, Japan,* [2]*Human Science and Environment, University of Hyogo Graduate School, Hyogo, Japan,* [3]*Laboratory of Clinical Nutrition, Department of Food Science and Nutrition, Kinki University Faculty of Agriculture, Nara, Japan*

Abstract : NaPi-IIc/SLC34A3 is a sodium-dependent inorganic phosphate (Pi) transporter in the renal proximal tubules and its mutations cause hereditary hypophosphatemic rickets with hypercalciuria (HHRH). In the present study, we created a specific antibody for opossum SLC34A3, NaPi-IIc (oNaPi-IIc), and analyzed its localization and regulation in opossum kidney cells (a tissue culture model of proximal tubular cells). Immunoreactive oNaPi-IIc protein levels increased during the proliferative phase and decreased during differentiation. Moreover, stimulating cell growth upregulated oNaPi-IIc protein levels, whereas suppressing cell proliferation downregulated oNaPi-IIc protein levels. Immunocytochemistry revealed that endogenous and exogenous oNaPi-IIc proteins localized at the protrusion of the plasma membrane, which is a phosphatidylinositol 4,5-bisphosphate (PIP_2) rich-membrane, and at the intracellular vacuolar membrane. Exogenous NaPi-IIc also induced cellular vacuoles and localized in the plasma membrane. The ability to form vacuoles is specific to electroneutral NaPi-IIc, and not electrogenic NaPi-IIa or NaPi-IIb. In addition, mutations of NaPi-IIc (S138F and R468W) in HHRH did not cause cellular PIP_2-rich vacuoles. In conclusion, our data anticipate that NaPi-IIc may regulate PIP_2 production at the plasma membrane and cellular vesicle formation. J. Med. Invest. 62 : 209-218, August, 2015

Keywords **:** *proximal tubule, SLC34A3, opossum kidney cells, proliferation, vacuole*

INTRODUCTION

Inorganic phosphate (Pi) homeostasis in the body is mediated by the absorption of dietary Pi in the small intestine, reabsorption from the urine into the kidney, and bone formation/resorption. Type II Na^+-dependent Pi (NaPi) cotransporters (SLC34A1/Npt2a/NaPi-IIa, and SLC34A3/Npt2c/NaPi-IIc) and type III NaPi cotransporter (PiT-2/Slc20a2) are expressed at the apical membrane of the proximal tubular cells and mediate Pi transport (1, 2). Type II NaPi transporters in the renal proximal tubules mediate the rate-limiting step in overall-Pi reabsorption (3, 4). The type II NaPi family comprises electrogenic NaPi-IIa/b and electroneutral NaPi-IIc, which have Na^+ : Pi cotransport stoichiometries of 3 : 1 and 2 : 1, respectively (5, 6). NaPi-IIa and NaPi-IIc are major functional transporters in the apical membrane of the proximal tubular cells (1, 2). In rodents, NaPi-IIa is the most important renal Pi cotransporter, and NaPi-IIa-knockout (KO) mice have hypophosphatemia and hyperphosphaturia (7). In contrast, NaPi-IIc is a major functional NaPi cotransporter in the human kidney, because NaPi-IIc mutations cause hereditary hypophosphatemic rickets with hypercalciuria (HHRH) (8, 9). Individuals affected by HHRH who carry compound heterozygous or homozygous (com/hom) NaPi-IIc mutations exhibit increased urinary Pi excretion, leading to hypophosphatemic rickets, bowing, and short stature, as well as elevated 1,25 $(OH)_2$ D_3 levels (8-10).

Received for publication May 21, 2015 ; accepted June 1, 2015.

Address correspondence and reprint requests to Ken-ichi Miyamoto PhD Department of Molecular Nutrition Institute of Biomedical Sciences Tokushima University Graduate School Tokushima, Japan 3-18-15 Kuramoto-cho, Tokushima 770-8503, Japan and Fax : +81-88-633-7081.

In a previous study using mouse models, we reported that NaPi-IIc plays a minor role in renal Pi reabsorption, and that NaPi-IIa may be able to sufficiently support NaPi cotransport activity to compensate for NaPi-IIc deficiencies in NaPi-IIc-KO mice (1, 11-13). The marked differences in the phenotypes of NaPi-IIa-KO and NaPi-IIc-KO mice may be due to the differential dominance in transporters for Pi homeostasis (7, 13, 14). Indeed, kidney expression of NaPi-IIc is high during weaning, but lower in adult animals (1, 11, 12). Furthermore, expression of NaPi-IIa transcripts is restricted to the proximal tubules (15), while NaPi-IIc transcripts are expressed in various tissues (e.g. intestine, spleen, testis, uterus, placenta, bone, and brain) (16).

Renal Pi transport is regulated by changes in the abundance of NaPi-IIa and NaPi-IIc proteins in the brush border membrane, and involves their interaction with scaffolding and signaling proteins essential to their brush border membrane insertion, retrieval, and degradation (2). Regulation by NaPi-IIc has been studied in less detail, however, because renal proximal tubular cells that express endogenous NaPi-IIc protein are not available.

Cellular cascades involved in the "physiologic/pathophysiologic" control of Pi reabsorption have been explored in a tissue culture model (opossum kidney [OK] cells) expressing intrinsic NaPi-IIa (NaPi-4) (17-21). As OK cells provide a "proximal tubular" environment, this tissue culture model is useful for characterizing (in heterologous expression studies) the cellular/molecular requirements for transport regulation (2). In previous studies, we investigated NaPi-IIc regulation in a heterologous expression system of OK cells (22, 23). In the present study, we created specific antibodies to opossum NaPi-IIc (oNaPi-IIc) and analyzed their localization. The levels of oNaPi-IIc protein were increased in proliferative cells, but not in differentiated cells. We discuss the physiological roles

of endogenous NaPi-IIc in OK cells.

MATERIALS AND METHODS

Plasmid constructs.

Full-length wild-type (WT) human NaPi-IIc, mouse NaPi-IIc, human NaPi-IIa, and mouse NaPi-IIb with a FLAG tag (pCMV-Tag2A vector ; Stratagene, La Jolla, CA ; FLAG-NaPi-IIc) or an enhanced green fluorescent protein (EGFP) tag (pEGFP-C1 vector ; Clontech, Palo Alto, CA ; EGFP-NaPi-IIa, EGFP-NaPi-IIc) or a mCherry tag (pmCherry-C1 vector ; Clontech ; mCherry-NaPi-IIc) at the NH_2 terminus were generated using standard cloning techniques (20, 22). PCR and a site-directed mutagenesis kit (QuikChange Lightning site-directed mutagenesis kit, Stratagene) were used to introduce the S138F and R468W mutations into EGFP-human NaPi-IIc WT, as previously described (23), and the S189 A, S191A, and G195D (electrogenic mutant) into EGFP- or FLAG-mouse NaPi-IIc WT (24). All human NaPi-IIc mutant cDNAs were subcloned into pCMV-Tag2A (Stratagene) for Pi uptake assays. Mouse NaPi-IIc electrogenic mutant constructs were confirmed by the following sequencing : S189A, S191A, G195D, 5'-cagagggccttcgccggcgcggccgtgcatg-3' (sense), 5'-catgcacggccgcgccggcgaaggccctctg-3' (antisense), and 5'-cgcggccgtgcatgacatcttcaactggc-3' (sense), 5'-gccagttgaagatgtcatgcacggccgcg-3' (antisense). PLCδ1PH domain-pEGFP-C1 (PLCδPH-EGFP) was kind gift from Dr. M. Isshiki (University of Tokyo, Tokyo, Japan) (25, 26).

Animals.

Mice were maintained under pathogen-free conditions and handled in accordance with the Guidelines for Animal Experimentation of Tokushima University School of Medicine. Male C57BL/6J mice were purchased from Charles River Laboratories Japan (Yokohama, Japan). NaPi-IIa KO mice were purchased from Jackson Laboratories (Bar Harbor, ME). The generation of NaPi-IIc KO mice was described previously (13).

Cell culture and plasmid transfection.

OK cells were obtained from the American Type Culture Collection (ATCC ; Rockville, MD) and 3B/2 clones were a kind gift from Dr. J. Biber (Zurich University, Switzerland, Switzerland). The OK cells were maintained in an appropriate medium (20). For live cell imaging, 1.4×10^5 cells/dish were plated in 35-mm glass-base dishes (Iwaki, Chiba, Japan) and subconfluent cultures were transfected with each EGFP- or mCherry-fused construct. For immunostaining, 0.5×10^5 cells/well were plated on glass coverslips (Matsunami-glass, Osaka, Japan) in 12-well dishes, and subconfluent cultures were transfected with a FLAG-fused construct. Transfections were performed for 24 h using LipofectAMINE® 2000 (Invitrogen, Carlsbad, CA) according to the manufacturer's instructions. For Western blotting analysis, 1.4×10^5 cells/well were plated in six-well dishes, and total cell lysates were prepared on days 2, 3, 4, and 6 after seeding.

Reverse transcription-PCR analysis.

Total RNA was prepared from OK cells using ISOGEN (Nippon Gene, Tokyo, Japan) (22). cDNA was synthesized using the Moloney murine leukemia virus, reverse transcriptase (Superscript, Invitrogen), and Oligo (dT) 12-18 Primer. PCR was initiated with denaturation at 98°C for 3 min, followed by amplification at 95°C for 30 s, 57-60°C for 30 s, and 72°C for 30 s for 25 to 35 cycles. Primers used in this study are listed in Table 1.

Pi uptake studies in OK cells.

Pi transport was studied in monolayers of OK cells transfected with each FLAG-fused construct in 12-well dishes. Uptake experiments were performed as previously described (22, 23). In brief, Pi uptake studies were carried out in uptake solution containing 137 mM NaCl, 5.4 mM KCl, 2.8 mM $CaCl_2$, 1.2 mM $MgSO_4$, 10 mM HEPES-Tris (pH 7.4), 0.1 mM KH_2PO_4/K_2HPO_4, and 1 μCi/ml ^{32}P (PerkinElmer, Bridgeport, CT) at 37°C. After 6 min, the cells were washed three times with cold stop solution containing 137 mM NaCl, 10 mM Tris-HCl pH 7.2, 2 mM KH_2PO_4/K_2HPO_4 (pH 7.4), and then solubilized by the addition of 0.4 ml of 0.1 N NaOH. Insta-Gel Plus (PerkinElmer) was added to the cell lysates. ^{32}P levels in cell lysates were determined using a bicinchoninic acid assay protein assay kit (Pierce, Rockford, IL). Pi transport was calculated as nanomoles ^{32}P per milligram protein taken up in 6 min. These experiments were performed in triplicate and repeated two to four times.

Preparation of rabbit polyclonal anti-oNaPi-IIc antibody.

An amino acid peptide sequence from the carboxyl-terminal (CFENPVVLASQRL) of oNaPi-IIc was fused to keyhole limpet hemocyanin, and used to generate rabbit polyclonal antibody by Medical and Biological Laboratories (Aichi, Japan) (22, 23).

Confocal microscopy analysis.

Cells were imaged using an A1R confocal laser scanning microscope system (Nikon, Tokyo, Japan) equipped with a 60× oil immersion objective. Immunostaining was performed as described previously (22, 23). For protein detection, cells were incubated with anti-NaPi-4 (oNaPi-IIa) polyclonal (1 : 100), anti-oNaPi-IIc polyclonal (1 : 100), or anti-FLAG-M2 monoclonal antibody (Sigma, 1 : 250). Alexa Fluor 568-Phalloidin (Molecular Probes, Eugene, OR ; 1 : 100) was used for the detection of actin. Alexa Fluor 488-conjugated mouse IgG (Molecular Probes, 1 : 100), or Alexa Fluor 488-conjugated rabbit IgG (Molecular Probes, 1 : 100) was used as the secondary antibody. Coverslips were mounted with Aqua PolyMount (Polysciences, Warrington, PA).

Table 1
primers used in this study

	Gene	Sense (5'-3')	Antisense (5'-3')	Product size (bp)	Reference
RT-PCR	oNaPi-IIa	GCTGGCTCCCTTACCCTACTG	GATGACTGTCTGGACCACCTTG	102	L26308 (NCBI Nucleotide)
	oNaPi-IIc	GGTGGTGGGAGCCTTTACTC	TTTGGTCATGTTGCCTGTGG	139	XM_007475445
	PiT-1	GGTGGGAACGATGTCAGCAA	ACCAACGCCACCATACAACA	123	XM_007477569
	PiT-2	TGATACCACCATTCCCCTCA	AACCGTGCGTCATGGAAAG	119	XM_001373110
	Megalin	AGGCTCCCTTCTGCCATCTCTTC	GCAGAATCTGGTCCAAAACCTGACAC	144	Endocrinology. 2009 Feb ; 150(2) : 871-8.
	GAPDH	CTGCACCACCAACTGCTTAGC	GCCTGCTTCACCACCTTCTTG	342	Am J Physiol Renal Physiol 2010 Jul : 299(1) : F243-54.

Preparation of total cell lysates.

Proteins were isolated as described previously (22, 23). OK cells were rinsed twice with ice-cold Tris-buffered saline, scraped off in the isolation buffer (0.5% nonidet P-40, 1 mM PMSF, 2 μg/ml aprotinin, and 2 μg/ml leupeptin in Tris-buffered saline (pH 7.5) and resuspended five times using a 20-gauge needle. Homogenates were centrifuged at 10,000× g for 2 min, and supernatants were collected in new tubes. The protein concentration in the lysates was determined using a bicinchoninic acid protein assay kit (Pierce) and analyzed by Western blotting.

Preparation of BBMV and whole homogenate for immunoblotting.

Brush border membrane vesicles (BBMVs) were prepared from the kidneys from the mice using the Ca^{2+} precipitation methods described as previously (13, 27). Kidney was sliced and thoroughly homogenized in homogenate buffer (5 mM Tris-HCl/ pH 7.5, 250 mM sucrose, 0.1 mM phenylmethylsulfonyl fluoride). The homogenate was centrifuged at 3000 rpm for 10 minutes. The supernatant was used for whole homogenate sample.

Immunoblot analysis.

Cells grown on 6-wells were transfected as described above and previously (22, 23). In brief, equivalent amounts of protein samples were heated at 95°C for 3 min in sample buffer containing 5% 2-mercaptoethanol, subjected to 9% SDS-PAGE, and transferred electrophoretically to polyvinylidene difluoride transfer membranes (Immobilon-P ; Millipore, Billerica, MA). Membranes were incubated in 5% skim milk in 20 mM Tris-HCl (pH 7.5), 150 mM NaCl, and 0.1% Tween 20 (TBST) at room temperature for 1 h to inhibit nonspecific binding, and then overnight at 4°C with anti-oNaPi-IIc polyclonal (1 : 2000), anti-NaPi-4 (oNaPi-IIa) polyclonal (1 : 2000), anti-mouse NaPi-IIc polyclonal (1 : 1500), anti-proliferating cell nuclear antigen (PCNA) monoclonal (Sigma, P8825, 1 : 15000), anti-opossum Megalin polyclonal (a kind gift from Dr. A. Saito, Niigata University, Niigata, Japan ; 1 : 1000) (28) or anti-actin monoclonal antibody (Chemicon, Temecula, CA ; used as an internal control, 1 : 10000), in 1% skim milk in TBST, followed by treatment with horseradish peroxidase-conjugated secondary antibody (Jackson ImmunoResearch, West Grove, PA ; 1 : 10000). Signals were detected using the Immobilon Western detection system (Millipore).

Statistics.

Differences among multiple groups were analyzed by ANOVA. A P value of less than 0.05 was considered statistically significant.

RESULTS

Expression of NaPi-IIc protein in OK cells.

To investigate the expression of endogenous oNaPi-IIc protein in OK cells by Western blot, we produced polyclonal antibodies against the oNaPi-IIc carboxyl-terminus (C-terminus). Full length amino acid sequence of type IIc NaPi transporters in opossum (gray short-tailed opossum, NCBI Reference Sequence, XP_007475507.1) and human (NP_001170787.1) are 69% homologous. Furthermore, the amino acid sequence of the oNaPi-IIc C-terminus is highly conserved among mouse, human, and opossum (Fig. 1A), and XP_007475507.1 was used as the oNaPi-IIc amino acid sequence. The oNaPi-IIc protein was detected as ~ 80 kDa protein in OK cells (Fig. 1B). Anti-oNaPi-IIc antibody specificity was confirmed by the absence of bands of ~ 80 kDa in the competition assay using antibody incubated with antigen peptide (Fig. 1B). In contrast, HeLa cells did not express endogenous NaPi-IIc protein, based on Western blot analysis (data not shown). In addition, NaPi-IIc protein in wild-type (WT) and NaPi-IIa KO mouse kidney was recognized by anti-oNaPi-IIc antibody, whereas in NaPi-IIc KO mouse was not detected by anti-oNaPi-IIc antibody (Fig. 1C).

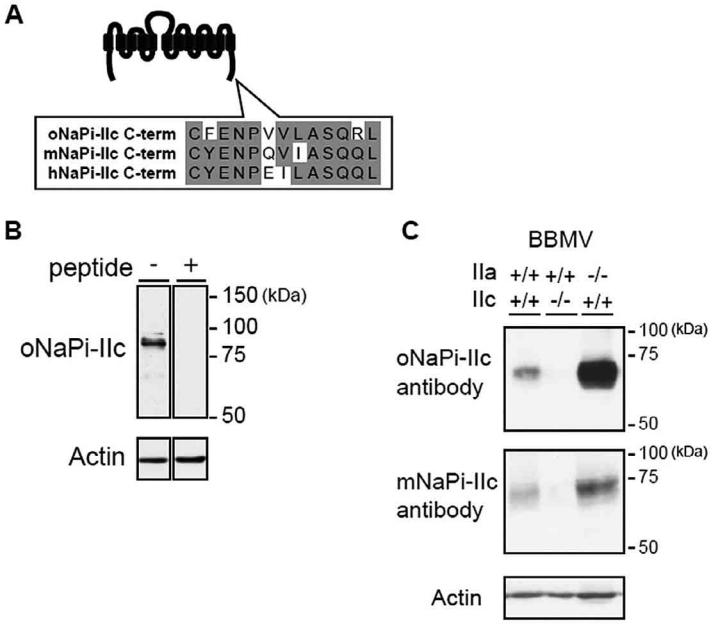

Fig. 1
Production and characterization of anti-oNaPi-IIc antibody **A** Alignment of the C-terminus 13-amino acid sequence of NaPi-IIc (opossum, mouse, human). **B** Peptide competition assay. Total cell lysates from OK cells at day 2 after seeding were separated by SDS-PAGE, and the blotted membrane was probed with anti-oNaPi-IIc antibody, which was preincubated for 1 h at room temperature with (+) or without (-) recombinant fragments corresponding to the 13-amino acid of the oNaPi-IIc C-terminus, as indicated. **C** Western blotting analysis using renal BBMV isolated from the kidney of WT, NaPi-IIc-KO (NaPi-IIc -/-), and NaPi-IIa-KO (NaPi-IIa -/-) mice by opossum and mouse NaPi-IIc antibodies. Actin was used as an internal control.

We then investigated the expression of endogenous oNaPi-IIa and oNaPi-IIc proteins during cell proliferation and differentiation. Total cell lysates and total mRNAs were obtained on days 2, 3, 4, and 6 after cell seeding (Fig. 2A). Microscopy analysis revealed that OK cells were sub-confluent at day 2, confluent at day 3, and formed domes (characteristic of proximal tubular cells) on day 5 (data not shown). Based on RT-PCR analysis, oNaPi-IIa (NaPi-4) mRNA levels increased throughout the differentiation phase (days 4, 6 ; Fig. 2B). The levels of Megalin mRNA, a marker of the differentiation of proximal tubular cells with a time-course of induction similar to that of oNaPi-IIa, were increased in OK cells on days 4 and 6 (Fig. 2B). oNaPi-IIc mRNA levels were also abundant in the differentiated phase (Fig. 2B). The PiT-1 and PiT-2 mRNA levels were unchanged in between proliferative and differentiated cells (Fig. 2B). Moreover, Pi transport activity was higher in the differentiated phase than in the proliferative phase (Fig. 2C). By Western blot analysis, expression of oNaPi-IIa protein was only detected in the differentiated phase (days 4, 6), and not the proliferative phase (days 2, 3) (Fig. 2D). Similarly to oNaPi-IIa protein expression, Megalin levels were higher in differentiated cells (days 4, 6) than in proliferative cells (days 2, 3 ; Fig. 2D). These observations are consistent with several previous reports (29). In contrast, the ~ 80 kDa protein bands of oNaPi-IIc protein were detected in the proliferative phase, and not in the differentiated phase (Fig. 2D). The oNaPi-IIc protein levels correlated with the expression of PCNA protein, which is a marker of the proliferative phase. Confocal microscopy revealed co-localization of the immunoreactive signals of oNaPi-IIa protein with F-actin at the apical patch in differentiated cells (day 6) (Fig. 2E), while immunoreactive signals of oNaPi-IIa were not detected in proliferative cells (day 2). In contrast, immunoreactive signals of oNaPi-IIc protein localized at the membrane protrusion (lamellipodia and cell membrane ruffles) at the leading edge of proliferative cells (day 2), and not in differentiated cells (day 6 ; Fig. 2E). Overexpressed human NaPi-IIc protein also localized at the protrusion (cell membrane ruffles, Fig. 2F) and induced cellular vacuoles (data not shown).

Effect of cell cycle synchronization and release on NaPi-II expression.

We then analyzed the expression of oNaPi-IIc in OK cells that were synchronized by serum starvation (for 2 days), and then released by serum re-feeding for 4, 8, 12, 16, 20, and 24 h (Fig. 3A). The cell cycle profiles were analyzed by flow-cytometry (Fig. 3B). The rates of cells in G_0/G_1 phases were increased by serum starvation, and the rates of cells in $S+G_2/M$ phases were increased in cells with serum re-feeding after serum starvation (Fig. 3B). oNaPi-IIa protein levels were increased in serum-starved cells synchronized in the G_0/G_1 phase, and downregulated in serum re-fed cells entering the cell cycle (Fig. 3B, C). Megalin protein levels were similar to those of oNaPi-IIa protein (Fig. 3C). In contrast, oNaPi-IIc protein levels were downregulated in the serum-starved cells, and increased in the serum re-fed cells (Fig. 3C). These findings indicate that oNaPi-IIc protein levels increase in proliferative cells entering the cell cycle in the presence of serum. Immunocytochemistry revealed oNaPi-IIa protein signals at apical patches in the serum-starved cells (Fig. 3D), but not in serum re-fed cells. By contrast, oNaPi-IIc protein was not observed in serum-starved cells, but were clearly detected at the plasma membrane (protrusion) and cellular vesicles in the serum re-fed cells (Fig. 3D). These findings suggest that oNaPi-IIc is induced by the stimulation of proliferation in OK cells.

Effect of NaPi-IIc on vacuole formation in OK cells.

Next, we investigated whether NaPi-IIc expression affects the formation of cell membrane protrusions. As shown in Fig. 4A, overexpressed human NaPi-IIc, but not human NaPi-IIa or mouse NaPi-IIb (data not shown), induces the formation of membrane protrusions and cellular vacuoles. Vacuoles in proximal tubular cells are often observed as endosomes, which have a role in the endocytosis of various substrates, such as albumin, vitamin D-binding protein, and transferrin (30-32). Endocytosis is regulated by many phospholipids containing phosphatidylinositol 4,5-bisphosphate (PIP_2) (33). The oNaPi-IIc localized with PLCδPH-EGFP (PIP_2 marker) at the membrane (Fig. 4B), and overexpressed NaPi-IIc co-localized with PLCδPH-EGFP at the cell surface and in PIP_2-rich cellular vacuoles (Fig. 4C).

Effect of HHRH mutations on NaPi-IIc function in OK cells.

The oNaPi-IIc localized in the protrusion and cellular vesicles, and overexpression of NaPi-IIc induced PIP_2-rich vacuoles under the plasma membrane (Fig. 4B, C). These findings suggest that NaPi-IIc is involved in PIP_2 production. Indeed, overexpression of PLCδPH-EGFP induces cellular vacuoles as reported previously (34). We then investigated whether the production of cellular vacuoles is due to the properties of NaPi-IIc (electroneutral NaPi cotransport activity) (24). We constructed the electrogenic NaPi-IIc mutant as reported previously (24) and analyzed whether electrogenic NaPi-IIc induces cellular vacuoles in OK cells. Overexpression of NaPi-IIc (WT) induced Pi transport activity and cellular vacuoles (Fig. 5A, B). In contrast, electrogenic NaPi-IIc did not induce the formation of cellular vacuoles in the transfected OK cells (Fig. 5A, B). These findings indicate that expression of the electroneutral NaPi cotransporter could induce cellular vacuoles in OK cells. Moreover, we investigated whether NaPi-IIc with HHRH mutations affected the formation of cellular vacuoles in OK cells. The WT human NaPi-IIc markedly increased NaPi cotransport activities in OK cells, while mutations (S138F, R468W) of NaPi-IIc markedly suppressed NaPi cotransport activities (Fig. 5C). In addition, NaPi-IIc WT stimulated the formation of cellular vacuoles, while NaPi-IIc mutants (S138F and R468W) failed to induce cellular vacuole formation (Fig. 5D). These findings indicate that NaPi-IIc with HHRH mutations decreases both vacuole formation and NaPi cotransport activity.

DISCUSSION

In the present study, we investigated the expression of endogenous NaPi-IIc (oNaPi-IIc) in OK cells using specific antibodies. Immunoreactive signals of oNaPi-IIc increased in growth conditions and markedly decreased in the differentiated phase. Using confocal image analysis, we detected immunoreactive signals of oNaPi-IIc in the plasma membrane and cellular vesicles in undifferentiated OK cells. Regulation of oNaPi-IIc might be involved in post-translational modification or the control of protein degradation, based on the high levels of oNaPi-IIc mRNA transcripts in differentiated OK cells.

Serum starvation prevents the proliferation of various cells and refeeding of serum stimulates cell proliferation (35). Under these conditions, the expression profiles of oNaPi-IIa and oNaPi-IIc in OK cells differed markedly. The oNaPi-IIc levels were increased by stimulating cell proliferation.

In the proliferative phase, oNaPi-IIc localized in the membrane protrusion and cellular vesicles. We analyzed the localization in proliferative OK cells using FLAG-tagged exogenous NaPi-IIc (human or mouse). The localization of exogenous NaPi-IIc was almost identical to that of oNaPi-IIc in OK cells. Exogenous NaPi-IIc induced cellular vacuoles and localized in the plasma membrane. These expression patterns were very similar to those of PIP_2 expression, which induces protrusions or membrane vesicle trafficking. Furthermore, the vacuole formation ability may be specific to NaPi-IIc, but not NaPi-IIa and NaPi-IIb. Indeed, the electrogenic

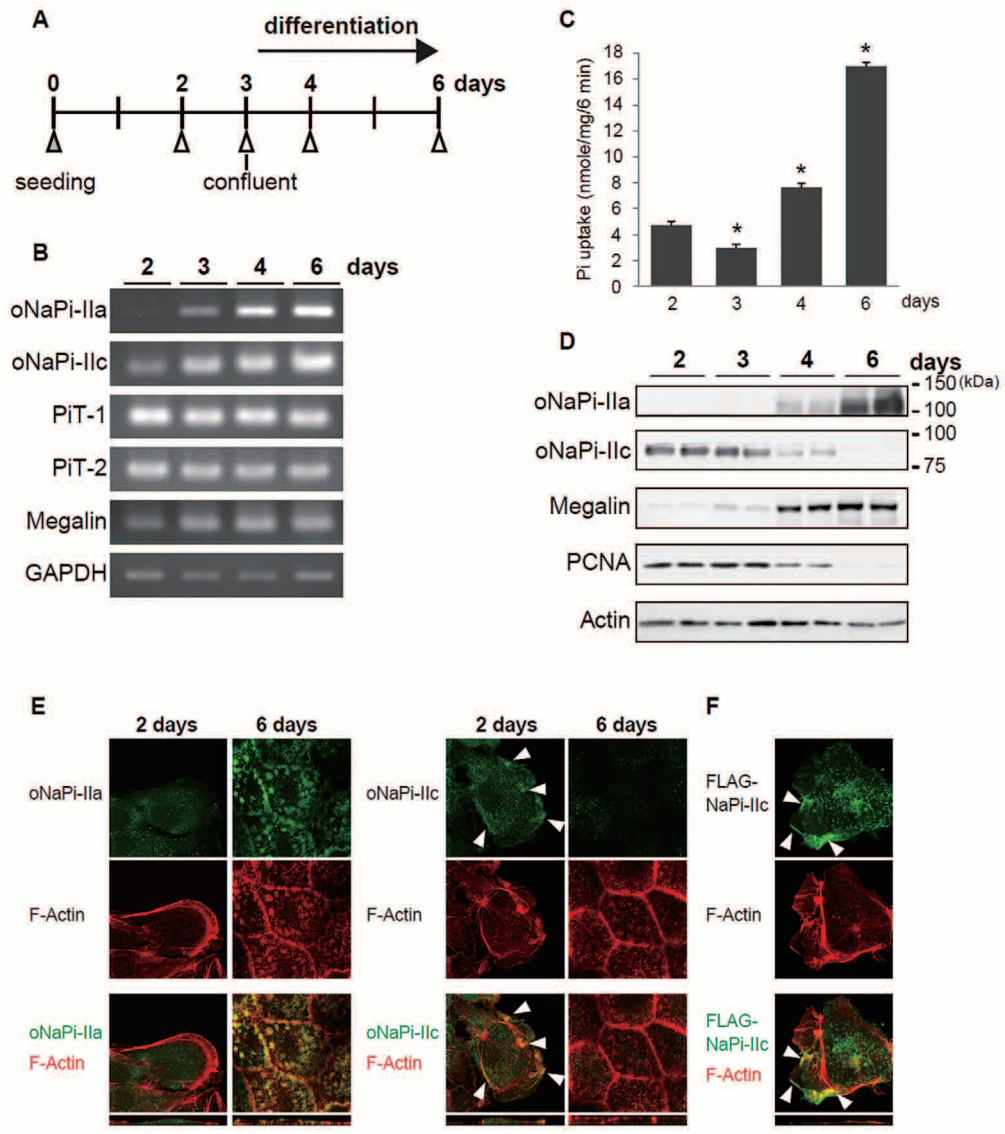

Fig. 2
Expression of NaPi-4 (oNaPi-IIa) and endogenous oNaPi-IIc in OK cells. **A** Schematic of the experiment schedule. OK cells were plated, and total cell lysates or total mRNAs were prepared on days 2, 3, 4, and 6 after seeding. **B** Levels of oNaPi-IIa and oNaPi-IIc and type III NaPi cotransporter (PiT-1 and PiT-2) mRNAs were assessed by RT-PCR analysis. Gapdh mRNA was amplified as an internal control. **C** Monolayers of OK cells were seeded in 12-well dishes, and Pi uptake was examined on days 2, 3, 4, and 6 after seeding. Results are expressed as means±SE (n=3) of uptake values. *$P<0.05$ vs. day 2. **D** Expression of oNaPi-IIa and oNaPi-IIc protein in OK cells was analyzed by Western blot analysis. PCNA was used as a cellular marker of cell proliferation. Megalin was used as a marker of the differentiation of proximal tubular cells. Actin was used as an internal control. **E** Localization of oNaPi-IIa and oNaPi-IIc in proliferative (2 days) or differentiated (6 days) cells was analyzed by indirect immunofluorescence. Cells were fixed and stained with antibody against oNaPi-IIa or oNaPi-IIc and F-actin (Phalloidin). In merged images, oNaPi-IIa and oNaPi-IIc are shown in green, F-actin is shown in red, and the overlay of both signals is shown yellow. Arrowheads indicate localization of NaPi-IIc protein with F-actin. The xz cross-section is indicated in the lower panels. **F** Localization of NaPi-IIc in transiently transfected proliferative OK cells was analyzed by indirect immunofluorescence. OK cells transfected with FLAG-NaPi-IIc were stained with antibodies against FLAG and F-actin. In merged images, FLAG-NaPi-IIc is shown in green, F-actin is shown in red, and the overlay of both signals is shown yellow. Arrowheads indicate localization of NaPi-IIc protein with F-actin. The xz cross-section is indicated in the lower panels.

NaPi-IIc mutant caused no cellular vacuole formation.

Cell migration involves the transient formation of membrane protrusions (lamellipodia and cell membrane ruffles) at the leading edge of the cell ; these are thought to require rapid local changes in ion fluxes and cell volume (36). We postulated that NaPi-IIc expression alters the rate of the formation of cell membrane protrusions. NaPi-IIc might accelerate cell migration by facilitating the rapid turnover of cell membrane protrusions at the leading edge. It has been proposed that actin cleavage and ion uptake at the tip of a lamellipodium create local ion gradients that drive the influx of phosphate ions across the cell membrane (36).

HHRH is characterized by hypophosphatemia secondary to renal Pi wasting, resulting in increased serum 1, 25 $(OH)_2$ D_3 concentrations with associated intestinal Ca^{2+} hyperabsorption, hypercalciuria, rickets, and osteomalacia (8-10). In patients with HHRH, the mechanism underlying the increased vitamin D synthesis in the proximal tubules is unknown. It is reported that vitamin D synthesis increases due to endocytic abnormalities in the renal proximal

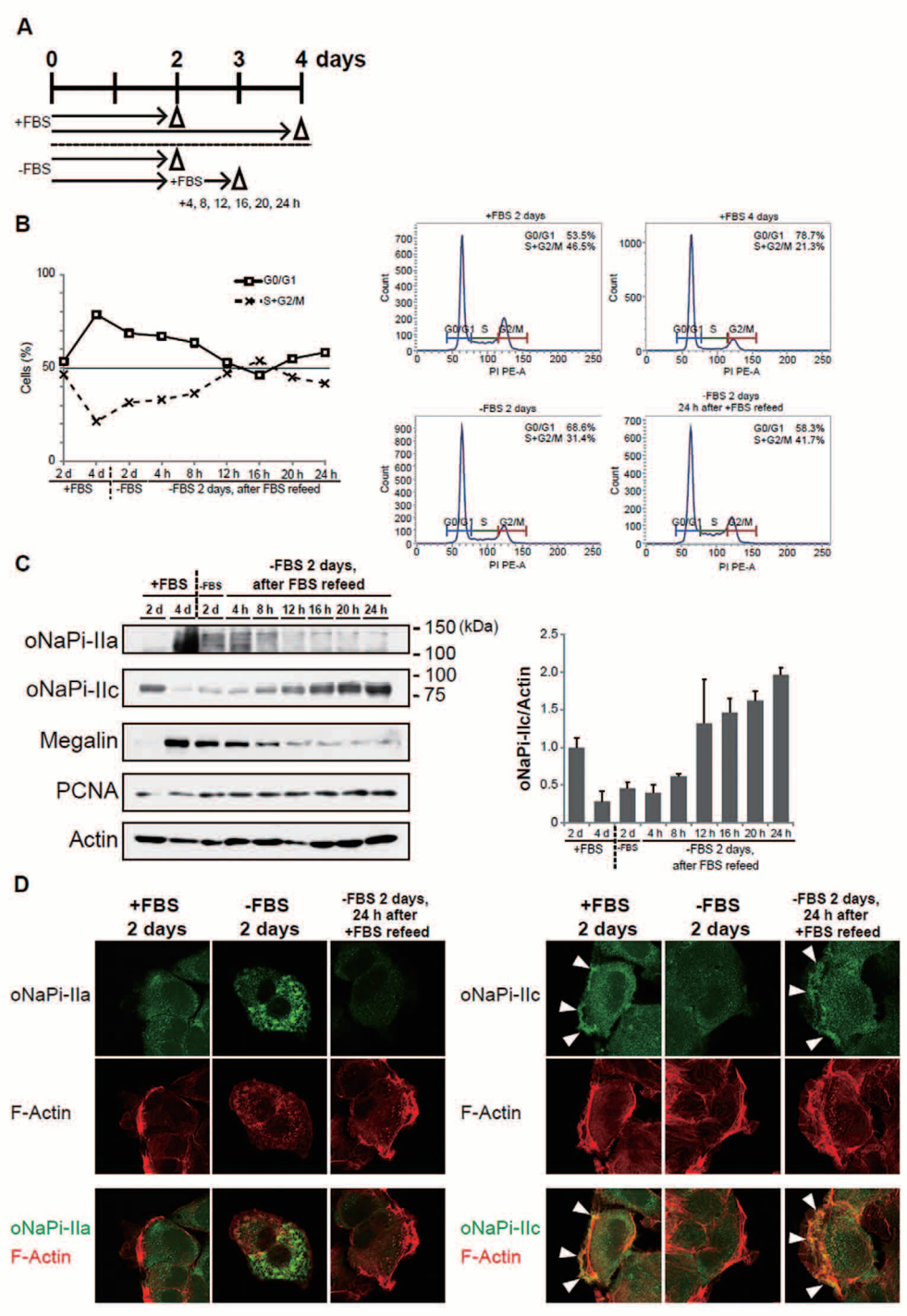

Fig. 3

Effects of serum starvation and re-feeding on the expression of oNaPi-IIa and oNaPi-IIc. **A** Schematic of the experiment schedule. OK cells were cultured in media with 0.1% bovine serum albumin (serum starvation). After 48 h, media was replaced with DMEM containing 10% FBS (serum re-feeding), Total cell lysates were prepared every 4 h after medium change. Control cells were cultured in media with 10% FBS, and total lysates were prepared at days 2 (proliferation) and 4 (differentiation) after seeding. **B** Cell cycle profiles based on fluorescence-activated cell sorting analysis. DNA contents in asynchronous cells (cultured with 10% FBS for 2 or 4 days ; proliferative and differentiated cells as controls) and synchronous cells such as serum-starved cells for 2 days and 24 h after serum re-feeding are shown as histograms (right). Time-course of differentiation rates of cells at G_0/G_1 phases and proliferation rates of cells at $S+G_2/M$ phases in these DNA profiles are represented by a line graph (left). **C** Expression of oNaPi-IIa and oNaPi-IIc under serum starvation or re-feeding conditions was analyzed by Western blot. PCNA was used as a cellular marker of cell proliferation. Megalin was used as a marker of the differentiation of proximal tubular cells. Actin was used as an internal control. Band density is normalized against that of actin and expressed as relative intensity to that of the control (+FBS 2 days) levels. Means±SE from two to four independent experiments performed in duplicate are shown. **D** Localization of oNaPi-IIa and oNaPi-IIc under serum starvation or re-feeding conditions was analyzed by indirect immunofluorescence. Cells were fixed and stained with antibody against oNaPi-IIa or oNaPi-IIc and F-actin. In merged images, oNaPi-IIa and oNaPi-IIc are shown in green, F-actin is shown in red, and the overlay of both signals is shown yellow. Arrowheads indicate localization of oNaPi-IIc protein with F-actin.

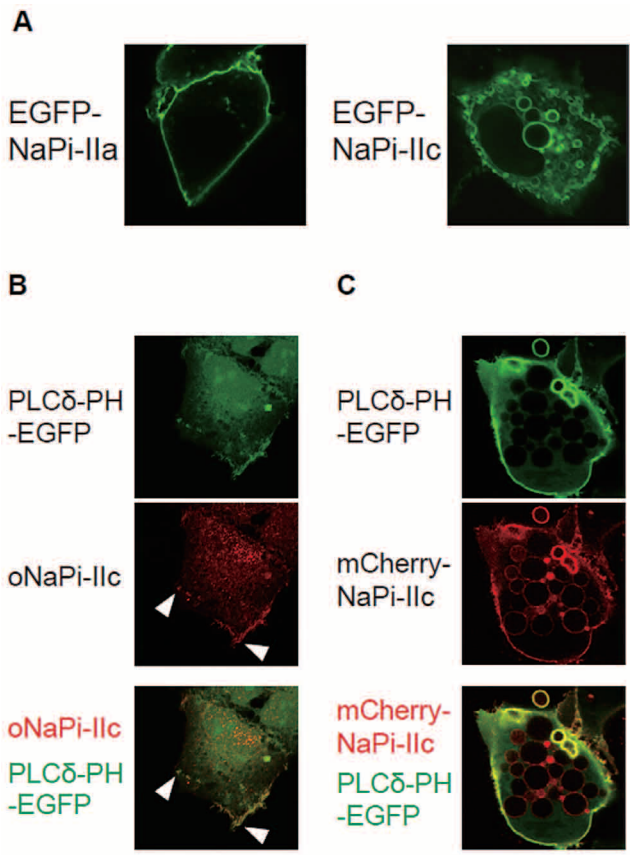

Fig. 4
Localization of NaPi-IIc and PLCδ-PH domains (PIP_2 marker) in proliferative OK cells was analyzed by indirect immunofluorescence. **A** Cellular vacuole formation was observed in OK cells transfected with EGFP-NaPi-IIa or NaPi-IIc. EGFP-NaPi-IIa or NaPi-IIc is shown in green. **B** OK cells transfected with PLCδPH-EGFP were stained with antibodies against NaPi-IIc. In merged images, oNaPi-IIc is shown in red, PLCδPH-EGFP is shown in green, and the overlay of both signals is shown yellow. Arrowheads indicate localization of oNaPi-IIc protein with PLCδPH-EGFP. **C** OK cells transfected with PLCδPH-EGFP and mCherry-NaPi-IIc were observed. In merged images, mCherry-NaPi-IIc is shown in red, PLCδPH-EGFP is shown in green, and the overlay of both signals is shown yellow.

tubules (37). Abnormal endocytosis in the proximal tubules is associated with mutations of genes such as CLC-5 (chloride/proton antiporter 5 [Dent's disease]) and OCRL (oculo-cerebro-renal syndrome of Lowe [Lowe syndrome]) (38-41). CLC-5 has a role in regulating intracellular endosomal pH-dependent activity to exchange endosomal luminal H^+ for cytosolic $2Cl^-$ (39). CLC-5 KO mice (Dent's disease model) exhibit hyperphosphaturia, hypercalciuria, and kidney stones due to endocytic dysfunction (38, 41, 42). The mutant mice show vitamin D deficiency, but increased vitamin D synthesis and downregulation of the degradation enzyme of vitamin D in the kidney (37). On the other hand, OCRL mediates membrane dynamics through PIP_2 phosphatase activity (43-46), and in vitro OCRL mutants failed to regulate intracellular vesicle transport. OCRL mutations also lead to cellular large vacuoles in various tissues.

In a previous study, vacuole formation was similar to that reported in ARF6-expressing epithelial cells (34). ARF6 influences cortical actin structures in the plasma membrane, lending support to the notion that membrane trafficking influences the composition and structure of the plasma membrane (34). ARF6 stimulates protrusion formation in the plasma membrane (34). Activation of ARF6 also induces the formation of PIP_2-positive actin-coated vacuoles that are unable to recycle membrane back to the plasma membrane (34). Overexpressed NaPi-IIc induced intracellular vacuolar formation and co-localization with PLCδPH-EGFP at the vacuolar membrane. PIP_2-rich membrane mediates both clathrin-dependent and independent endocytosis (33, 47), and is required for the uptake of urinary substrates and regulation of cell surface proteins in proximal tubular cells (48, 49). We hypothesize that NaPi-IIc is necessary for PIP_2 production and overexpression of NaPi-IIc activates ARF6 and enhances PIP_2 production. Furthermore, we demonstrated that HHRH mutants (S138F and R468W) do not form cellular vacuoles, suggesting that HHRH mutations affect PIP_2 production and vesicle transport.

Finally, in the present study, we are unable to elucidate the physiologic role of oNaPi-IIc in OK cells. The expression patterns of oNaPi-IIa and oNaPi-IIc were completely reversed during cell proliferation and differentiation. Expression of oNaPi-IIc increased during cell growth, and oNaPi-IIc localized in intracellular vesicles and in the membrane protrusion. These localization patterns suggest that NaPi-IIc is involved in cell migration and vesicle trafficking. Exogenous NaPi-IIc expression stimulates cellular vacuole formation in OK cells, suggesting that NaPi-IIc regulates intracellular vesicle transport by PIP_2 production. In addition, the present data indicate that HHRH mutations may affect PIP_2 production and vesicle transport. Further studies are needed, however, to clarify the mechanisms of cellular vacuole formation by NaPi-IIc.

ACKNOWLEDGMENTS

We thank Dr. Masashi Isshiki (University of Tokyo) for thoughtful comments and advice, Mitsuo Kitamura (Support Center for Advanced Medical Sciences, Institute of Biomedical Sciences, Tokushima University Graduate School) for technical assistance with FACS analysis, and appreciate the technical assistance from Division for bio-imaging, Support Center for Advanced Medical Sciences, Institute of Biomedical Sciences, Tokushima University Graduate School for the procedure of A1R confocal laser scanning microscope system.

GRANTS

This study was supported by Grants 25136715 and 26461253 (S. T.), 26461254 (H. S.), 26293204 (K. M.) from the Ministry of Education, Culture, Sports, Science and Technology of Japan.

DISCLOSURES

No conflicts of interest, financial or otherwise, are declared by the authors.

AUTHORS CONTRIBUTION

Y.S., H.S., A.O., and K.-I.M provided conception and design of the research ; Y.S., H.S., S.O., A.O., M.I., I.K., S.K., and S.T. performed the experiments ; Y.S., H.S., A.O., and K.-I.M. analyzed data ; Y.S., H.S. and K-.I.M. prepared the figures ; Y.S., H.S., K.-I.M drafted the manuscript.

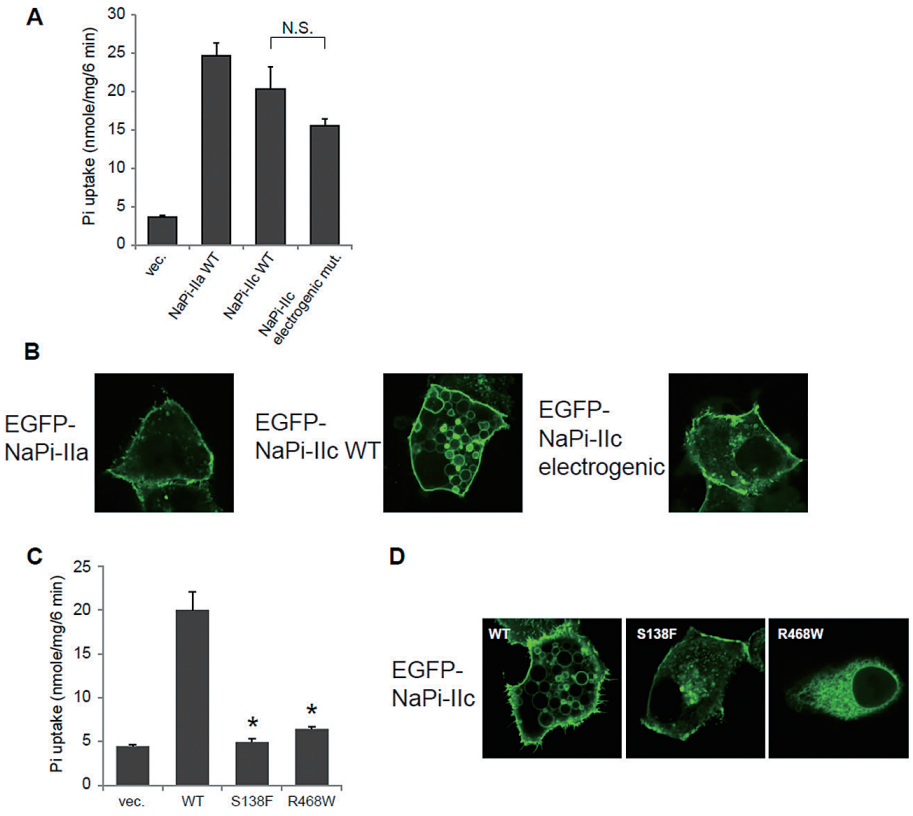

Fig. 5
Effects of electrogenic NaPi-IIc and HHRH mutations on vacuole formation in OK cells. **A** electrogenic NaPi-IIc mutant and Pi uptake. Pi uptake was assessed in OK cells transfected with empty vector (pCMV-Tag2A vec.) or FLAG-NaPi-IIa WT or NaPi-IIc (electroneutral) WT or electrogenic NaPi-IIc mutant (with S189A, S191A, G195D mutations). Results are expressed as means±SE (n=3) of uptake values. N.S. indicates nosignificant difference vs. FLAG-NaPi-IIc WT. **B** Cellular vacuole formation was observed in OK cells transfected with EGFP-NaPi-IIa or NaPi-IIc WT or electrogenic NaPi-IIc mutant. EGFP-NaPi-IIa or NaPi-IIc is shown in green. **C** HHRH mutants and Pi uptake. Pi uptake was assessed in OK cells transfected with empty vector (pCMV-Tag2A vec.) or FLAG-NaPi-IIc WT or NaPi-IIc with HHRH mutations (S138F or R468W). Results are expressed as means±SE (n=3) of uptake values. *$P<0.05$ vs. FLAG-NaPi-IIc WT. **D** Cellular vacuole formation by HHRH mutants was observed in OK cells transfected with EGFP-NaPi-IIc WT or NaPi-IIc with HHRH mutations (S138F or R468W). NaPi-IIc is shown in green.

REFERENCES

1. Segawa H, Kaneko I, Takahashi A, Kuwahata M, Ito M, Ohkido I, Tatsumi S, Miyamoto K : Growth-related renal type II Na/Pi cotransporter. J Biol Chem 277 : 19665-19672, 2002
2. Murer H, Hernando N, Forster I, Biber J : Proximal tubular phosphate reabsorption : molecular mechanisms. Physiol Rev 80 : 1373-1409, 2000
3. Biber J, Hernando N, Forster I, Murer H : Regulation of phosphate transport in proximal tubules. Pflugers Arch 458 : 39-52, 2009
4. Miyamoto K, Ito M, Tatsumi S, Kuwahata M, Segawa H : New aspect of renal phosphate reabsorption : the type IIc sodium-dependent phosphate transporter. Am J Nephrol 27 : 503-515, 2007
5. Forster IC, Loo DD, Eskandari S : Stoichiometry and Na+ binding cooperativity of rat and flounder renal type II Na+-Pi cotransporters. Am J Physiol 276 : F644-649, 1999
6. Miyamoto K, Haito-Sugino S, Kuwahara S, Ohi A, Nomura K, Ito M, Kuwahata M, Kido S, Tatsumi S, Kaneko I, Segawa H : Sodium-dependent phosphate cotransporters : lessons from gene knockout and mutation studies. J Pharm Sci 100 : 3719-3730, 2011
7. Beck L, Karaplis AC, Amizuka N, Hewson AS, Ozawa H, Tenenhouse HS : Targeted inactivation of Npt2 in mice leads to severe renal phosphate wasting, hypercalciuria, and skeletal abnormalities. Proc Natl Acad Sci U S A 95 : 5372-5377, 1998
8. Lorenz-Depiereux B, Benet-Pages A, Eckstein G, Tenenbaum-Rakover Y, Wagenstaller J, Tiosano D, Gershoni-Baruch R, Albers N, Lichtner P, Schnabel D, Hochberg Z, Strom TM : Hereditary hypophosphatemic rickets with hypercalciuria is caused by mutations in the sodium-phosphate cotransporter gene SLC34A3. Am J Hum Genet 78 : 193-201, 2006
9. Bergwitz C, Roslin NM, Tieder M, Loredo-Osti JC, Bastepe M, Abu-Zahra H, Frappier D, Burkett K, Carpenter TO, Anderson D, Garabedian M, Sermet I, Fujiwara TM, Morgan K, Tenenhouse HS, Juppner H : SLC34A3 mutations in patients with hereditary hypophosphatemic rickets with hypercalciuria predict a key role for the sodium-phosphate cotransporter NaPi-IIc in maintaining phosphate homeostasis. Am J Hum Genet 78 : 179-192, 2006
10. Yamamoto T, Michigami T, Aranami F, Segawa H, Yoh K, Nakajima S, Miyamoto K, Ozono K : Hereditary hypophosphatemic rickets with hypercalciuria : a study for the phosphate transporter gene type IIc and osteoblastic function. J Bone Miner Metab 25 : 407-413, 2007
11. Ohkido I, Segawa H, Yanagida R, Nakamura M, Miyamoto K : Cloning, gene structure and dietary regulation of the type-IIc Na/Pi cotransporter in the mouse kidney. Pflugers Arch

446 : 106-115, 2003
12. Kaneko I, Segawa H, Furutani J, Kuwahara S, Aranami F, Hanabusa E, Tominaga R, Giral H, Caldas Y, Levi M, Kato S, Miyamoto K : Hypophosphatemia in vitamin D receptor null mice : effect of rescue diet on the developmental changes in renal Na+-dependent phosphate cotransporters. Pflugers Arch 461 : 77-90, 2011
13. Segawa H, Onitsuka A, Kuwahata M, Hanabusa E, Furutani J, Kaneko I, Tomoe Y, Aranami F, Matsumoto N, Ito M, Matsumoto M, Li M, Amizuka N, Miyamoto K : Type IIc sodium-dependent phosphate transporter regulates calcium metabolism. J Am Soc Nephrol 20 : 104-113, 2009
14. Segawa H, Onitsuka A, Furutani J, Kaneko I, Aranami F, Matsumoto N, Tomoe Y, Kuwahata M, Ito M, Matsumoto M, Li M, Amizuka N, Miyamoto K : Npt2a and Npt2c in mice play distinct and synergistic roles in inorganic phosphate metabolism and skeletal development. Am J Physiol Renal Physiol 297 : F671-678, 2009
15. Magagnin S, Werner A, Markovich D, Sorribas V, Stange G, Biber J, Murer H : Expression cloning of human and rat renal cortex Na/Pi cotransport. Proc Natl Acad Sci U S A 90 : 5979-5983, 1993
16. Kuwahara S, Aranami F, Segawa H, Onitsuka A, Honda N, Tominaga R, Hanabusa E, Kaneko I, Yamanaka S, Sasaki S, Ohi A, Nomura K, Tatsumi S, Kido S, Ito M, Miyamoto K : Identification and functional analysis of a splice variant of mouse sodium-dependent phosphate transporter Npt2c. J Med Invest 59 : 116-126, 2012
17. Sorribas V, Markovich D, Hayes G, Stange G, Forgo J, Biber J, Murer H : Cloning of a Na/Pi cotransporter from opossum kidney cells. J Biol Chem 269 : 6615-6621, 1994
18. Pfister MF, Hilfiker H, Forgo J, Lederer E, Biber J, Murer H : Cellular mechanisms involved in the acute adaptation of OK cell Na/Pi-cotransport to high- or low-Pi medium. Pflugers Arch 435 : 713-719, 1998
19. Pfister MF, Lederer E, Forgo J, Ziegler U, Lotscher M, Quabius ES, Biber J, Murer H : Parathyroid hormone-dependent degradation of type II Na+/Pi cotransporters. J Biol Chem 272 : 20125-20130, 1997
20. Ito M, Iidawa S, Izuka M, Haito S, Segawa H, Kuwahata M, Ohkido I, Ohno H, Miyamoto K : Interaction of a farnesylated protein with renal type IIa Na/Pi co-transporter in response to parathyroid hormone and dietary phosphate. Biochem J 377 : 607-616, 2004
21. Nomura K, Tatsumi S, Miyagawa A, Shiozaki Y, Sasaki S, Kaneko I, Ito M, Kido S, Segawa H, Sano M, Fukuwatari T, Shibata K, Miyamoto K : Hepatectomy-related hypophosphatemia : a novel phosphaturic factor in the liver-kidney axis. J Am Soc Nephrol 25 : 761-772, 2014
22. Ito M, Sakurai A, Hayashi K, Ohi A, Kangawa N, Nishiyama T, Sugino S, Uehata Y, Kamahara A, Sakata M, Tatsumi S, Kuwahata M, Taketani Y, Segawa H, Miyamoto K : An apical expression signal of the renal type IIc Na+-dependent phosphate cotransporter in renal epithelial cells. Am J Physiol Renal Physiol 299 : F243-254, 2010
23. Haito-Sugino S, Ito M, Ohi A, Shiozaki Y, Kangawa N, Nishiyama T, Aranami F, Sasaki S, Mori A, Kido S, Tatsumi S, Segawa H, Miyamoto K : Processing and stability of type IIc sodium-dependent phosphate cotransporter mutations in patients with hereditary hypophosphatemic rickets with hypercalciuria. Am J Physiol Cell Physiol 302 : C1316-1330, 2012
24. Bacconi A, Virkki LV, Biber J, Murer H, Forster IC : Renouncing electroneutrality is not free of charge : switching on electrogenicity in a Na+-coupled phosphate cotransporter. Proc Natl Acad Sci U S A 102 : 12606-12611, 2005
25. Varnai P, Balla T : Visualization of phosphoinositides that bind pleckstrin homology domains : calcium- and agonist-induced dynamic changes and relationship to myo-[3H]inositol-labeled phosphoinositide pools. J Cell Biol 143 : 501-510, 1998
26. Isshiki M, Mutoh A, Fujita T : Subcortical Ca2+ waves sneaking under the plasma membrane in endothelial cells. Circ Res 95 : e11-21, 2004
27. Yusufi AN, Dousa TP : Studies on rabbit kidney brush border membranes : relationship between phosphate transport, alkaline phosphatase and NAD. Miner Electrolyte Metab 13 : 397-404, 1987
28. Hosojima M, Sato H, Yamamoto K, Kaseda R, Soma T, Kobayashi A, Suzuki A, Kabasawa H, Takeyama A, Ikuyama K, Iino N, Nishiyama A, Thekkumkara TJ, Takeda T, Suzuki Y, Gejyo F, Saito A : Regulation of megalin expression in cultured proximal tubule cells by angiotensin II type 1A receptor- and insulin-mediated signaling cross talk. Endocrinology 150 : 871-878, 2009
29. Lima WR, Parreira KS, Devuyst O, Caplanusi A, N'Kuli F, Marien B, Van Der Smissen P, Alves PM, Verroust P, Christensen EI, Terzi F, Matter K, Balda MS, Pierreux CE, Courtoy PJ : ZONAB promotes proliferation and represses differentiation of proximal tubule epithelial cells. J Am Soc Nephrol 21 : 478-488, 2010
30. Mattila PE, Raghavan V, Rbaibi Y, Baty CJ, Weisz OA : Rab 11a-positive compartments in proximal tubule cells sort fluid-phase and membrane cargo. Am J Physiol Cell Physiol 306 : C441-449, 2014
31. Cui S, Verroust PJ, Moestrup SK, Christensen EI : Megalin/gp330 mediates uptake of albumin in renal proximal tubule. Am J Physiol 271 : F900-907, 1996
32. Christensen EI, Birn H, Storm T, Weyer K, Nielsen R : Endocytic receptors in the renal proximal tubule. Physiology (Bethesda) 27 : 223-236, 2012
33. Jost M, Simpson F, Kavran JM, Lemmon MA, Schmid SL : Phosphatidylinositol-4,5-bisphosphate is required for endocytic coated vesicle formation. Curr Biol 8 : 1399-1402, 1998
34. Brown FD, Rozelle AL, Yin HL, Balla T, Donaldson JG : Phosphatidylinositol 4,5-bisphosphate and Arf6-regulated membrane traffic. J Cell Biol 154 : 1007-1017, 2001
35. Pardee AB : G1 events and regulation of cell proliferation. Science 246 : 603-608, 1989
36. Liu Q, Song B : Electric field regulated signaling pathways. Int J Biochem Cell Biol 55 : 264-268, 2014
37. Maritzen T, Rickheit G, Schmitt A, Jentsch TJ : Kidney-specific upregulation of vitamin D3 target genes in ClC-5 KO mice. Kidney Int 70 : 79-87, 2006
38. Christensen EI, Devuyst O, Dom G, Nielsen R, Van der Smissen P, Verroust P, Leruth M, Guggino WB, Courtoy PJ : Loss of chloride channel ClC-5 impairs endocytosis by defective trafficking of megalin and cubilin in kidney proximal tubules. Proc Natl Acad Sci U S A 100 : 8472-8477, 2003
39. Devuyst O : Dent's disease : chloride-proton exchange controls proximal tubule endocytosis. Nephrol Dial Transplant 25 : 3832-3835, 2010
40. Hichri H, Rendu J, Monnier N, Coutton C, Dorseuil O, Poussou RV, Baujat G, Blanchard A, Nobili F, Ranchin B, Remesy M, Salomon R, Satre V, Lunardi J : From Lowe syndrome to Dent disease : correlations between mutations of the OCRL1 gene and clinical and biochemical phenotypes. Hum Mutat 32 : 379-388, 2011
41. Piwon N, Gunther W, Schwake M, Bosl MR, Jentsch TJ : ClC-5 Cl--channel disruption impairs endocytosis in a mouse model for Dent's disease. Nature 408 : 369-373, 2000
42. Wang SS, Devuyst O, Courtoy PJ, Wang XT, Wang H, Wang Y, Thakker RV, Guggino S, Guggino WB : Mice lacking renal chloride channel, CLC-5, are a model for Dent's disease, a

nephrolithiasis disorder associated with defective receptor-mediated endocytosis. Hum Mol Genet 9 : 2937-2945, 2000
43. Erdmann KS, Mao Y, McCrea HJ, Zoncu R, Lee S, Paradise S, Modregger J, Biemesderfer D, Toomre D, De Camilli P : A role of the Lowe syndrome protein OCRL in early steps of the endocytic pathway. Dev Cell 13 : 377-390, 2007
44. Mao Y, Balkin DM, Zoncu R, Erdmann KS, Tomasini L, Hu F, Jin MM, Hodsdon ME, De Camilli P : A PH domain within OCRL bridges clathrin-mediated membrane trafficking to phosphoinositide metabolism. EMBO J 28 : 1831-1842, 2009
45. Ungewickell A, Ward ME, Ungewickell E, Majerus PW : The inositol polyphosphate 5-phosphatase Ocrl associates with endosomes that are partially coated with clathrin. Proc Natl Acad Sci U S A 101 : 13501-13506, 2004
46. Vicinanza M, Di Campli A, Polishchuk E, Santoro M, Di Tullio G, Godi A, Levtchenko E, De Leo MG, Polishchuk R, Sandoval L, Marzolo MP, De Matteis MA : OCRL controls trafficking through early endosomes via PtdIns4,5P(2)-dependent regulation of endosomal actin. EMBO J 30 : 4970-4985, 2011
47. Vicinanza M, D'Angelo G, Di Campli A, De Matteis MA : Function and dysfunction of the PI system in membrane trafficking. EMBO J 27 : 2457-2470, 2008
48. Gekle M : Renal tubule albumin transport. Annu Rev Physiol 67 : 573-594, 2005
49. Ramsammy LS, Josepovitz C, Lane B, Kaloyanides GJ : Effect of gentamicin on phospholipid metabolism in cultured rabbit proximal tubular cells. Am J Physiol 256 : C204-213, 1989